Mem. S.A.It. Vol. 81, 226

Memorie della

Progress in AGN research with XMM-Newton

M. Guainazzi

European Space Astronomy Centre of ESA, P.O.Box 78, Villanueva de la Cañada, E-28691, Madrid, Spain, e-mail: Matteo.Guainazzi@sciops.esa.int

Abstract. This paper reviews results obtained by the ESA observatory XMM-Newton in the field of Active Galactic Nuclei (AGN) research. I will cover six main areas: a) relativistic spectroscopy; b) soft excess; c) the quest for relativistic outflows; d) obscured AGN; e) scaling laws between Galactic and supermassive black holes, and f) AGN evolution and their contribution to the Cosmic X-ray Background.

Key words. Galaxies:active – Galaxies:nuclei – X-rays:galaxies

1. Introduction

By the time you read this paper, XMM-Newton Jansen et al. (2001) will have celebrated its 10^{th} anniversary in space. It was lunched on December 10^{th}, 1999, and since then it has been operating smoothly. At the end of September 2009, 2213 papers refereed paper using XMM-Newton data had been published. This numbers grows at a constant pace of about 300 publications per year. The average citation per paper is $\simeq$24.1 Trimble & Ceja (2008). Such a large scientific outcome has yielded a statistical basis large enough for a first assessment of the XMM-Newton astronomical legacy to be possible. A summary of this assessment in the specific Active Galactic Nuclei (AGN) research field is the main goal of this paper.

The XMM-Newton scientific payload comprises six instruments:

- three CCD cameras (EPIC, European Photon Imaging Camera). Two of then are based on MOS technology Turner et al. (2001), and one on pn devices Strüder et al. (2001). They allow imaging spectroscopy with moderate energy resolution (70–80 eV at 1 keV; $\simeq$150 eV at 6 keV). Each typical observations detects $\simeq$100 sources in the EPIC 30′ field of view, up to a sensitivity limit of the order of 10^{15} erg cm^{-2} s^{-1}. The fastest readout modes in the EPIC-pn reaches a time resolution of 7μs.
- two high resolution Reflection Grating Spectrometers (RGS, der Herder et al. 2001). They perform high-resolution (0.025–0.04Å) spectroscopy in the soft X-ray band (0.3–2 keV)
- one Optical Monitor telescope Mason et al. (2001), sensitive in the 1800-6000 Å wavelength range, and equipped with a series of lenticular filters in the optical (B,U,V) and UV band, as well as with grism systems which allow the measurements of spectra in the optical and UV

All the XMM-Newton instruments point simultaneously to the same region of the sky.

Send offprint requests to: M.Guainazzi

This allows astronomers to fully exploit their complementary properties, in particular the possibility of performing strictly simultaneous optical and X-ray observations.

Besides a continuously increasing number of pointed observations (≃6500 as of September 2009), three main catalogues are available to the science community and are being continuously updated:

- the 2XMM catalogue of serendipitous EPIC X-ray sources Watson et al. (2009). Its last version includes $\simeq 2.2\times10^5$ sources covering about 420 square degrees. About 80% of them are previously unknown. For about 45,000 of the brightest sources spectra and light curves are available with the catalogue. The median fluxes (in units of 10^{-14}erg cm^{-2} s^{-1}) are: 2.5, 0.6, and 1.4 in the 0.2–12, 0.2–2, and 2–10 keV energy band, respectively
- the Slew Catalogue Saxton et al. (2008), based on pn exposures taken during the spacecraft transit from one target to the next. This is a shallow wide-field (17000 square degrees as of September 2009, 14000 thereof at $|b| > 10^\circ$) survey. The median fluxes of the 7500 sources detected so far are 0.6 and 4×10^{-12} erg cm^{-2} s^{-1} in the 0.2–2 and 2–10 keV energy band, respectively
- the OM catalogue, including around 700000 sources with at least one UV filter measurement

More details about the XMM-Newton mission and its scientific products are available at the web page: `http://xmm.esac.esa.int`.

2. XMM-Newton recent contributions to our understanding of AGN

Any review paper on a subject as broad as AGN is unavoidably affected by personal taste and biases. I will try to minimise this risk by discussing in this paper the "most popular" topics in AGN astrophysics on the basis of an ADS-based list of papers (refereed journals only) discussing XMM-Newton data. It goes without saying that this paper does not have the ambition of being complete, exhaustive or representative in any sense.

2.1. Relativistic spectroscopy

Under this section I discuss measurements of the emission line profile distortion caused by the combination of kinematic and general relativistic effects Fabian et al. (1989); Matt et al. (1992); Miller (2007) in an X-ray illuminated accretion disk. After the first discovery by ASCA Tanaka et al. (1995), the launch of XMM-Newton, with its unprecedented and unsurpassed throughput in the hard X-ray band, fostered strong hopes that it would be possible to accurately measure relativistically broadened profiles of the iron K_α fluorescent line (and possibly of many others) in a large number of nearby AGN. The line profile depends on the disk inclination with respect to the line of sight; the location of innermost stable orbit (and therefore, indirectly, on the black hole spin); the radial emissivity profile (*i.e.* on the physics of the accretion flow); and the geometry of the high-energy emitting region. Its study may in principle allow to get insights on the accretion flow, as well as on two of the three "hairs" of cosmic supermassive black holes. Moreover, they might allow investigations of general relativity effects such as the light bending Martocchia et al. (2002); Miniutti & Fabian (2004) or the electromagnetic channel of energy extraction from a spinning black hole Blandford & Znajek (1977).

The reality proved much more controversial. Although measurements of relativistic profiles have been claimed in ≃30% of bright Seyferts Nandra et al. (2007) (cf. Fig. 1), none of these measurements has been exempt from severe scrutiny and criticisms. An alternative explanation for the broad red wing of the line profile, extending up to almost 1/2 of the nominal centroid rest frame energy Wilms et al. (2001); Turner et al. (2002); Fabian & Vaughan (2003); Dewangan et al. (2003) has been proposed in terms of the continuum curvature due to high-density, highly ionised outflows Reeves et al. (2004); Miller et al. (2007); Turner & Miller (2009) partially covering the

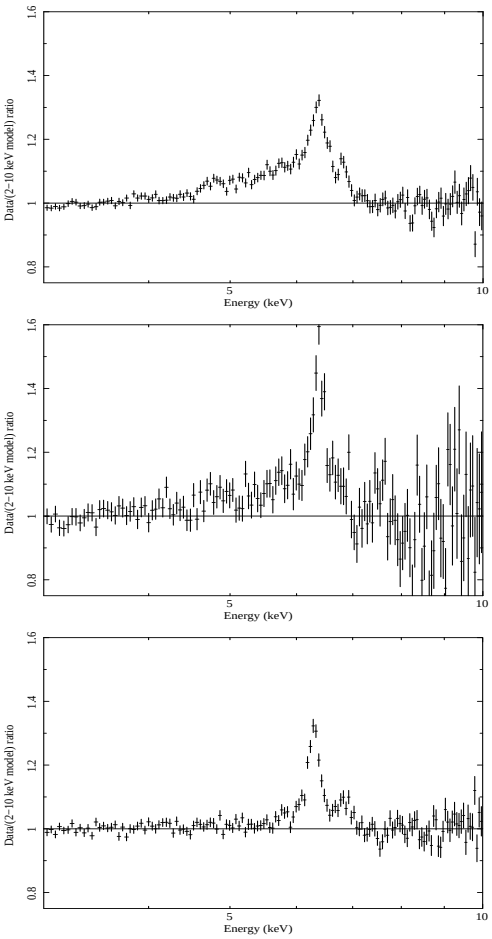

Fig. 1. EPIC-pn residuals (in units of data/model ratio) against the best-fit power-law model in the 2–10 keV energy band, once the 4–7 keV energy band has been removed prior to the fit. The broad and skewed excess emission in the 4–7 keV range is the phenomenological basis for the study of relativistic effects via X-ray spectroscopy in AGN (see Miller 2007 for a review). Form top to bottom: MCG-6-30-15 Wilms et al. (2001); Fabian & Vaughan (2003), NGC4051 Pounds et al. (2004), and IC 4329A Steenbrugge et al. (2005); Markowitz et al. (2006).

active nucleus. Controversy is fierce. Both scenarios yield comparably good statistical quality when applied to the same data, even if the absorption scenario has typically a larger number of free parameters, and require an anti-correlation between AGN output and absorber covering fraction for which there is no immediate explanation; (Miller et al. 2007). However, a recent result may have settled the issue (at least in one source!): the discovery of ≃30 s negative lag between the soft (0.3–1 keV) and the hard (1–4 keV) light curves in a 6-days long XMM-Newton observations of the Narrow Line Seyfert 1 Galaxy 1H0707-496 Fabian et al. (2009). The most natural explanation for this finding is in terms of the longer optical path that a photon reflected from the accretion disk needs to travel with respect to one directly emitted by the primary source. Thomas Boller discusses in more details this observation in this volume.

If the relativistic interpretation of broadened emission lines is correct, the door is open to measuring fundamental quantities of supermassive black holes in AGN. Brenneman & Reynolds (2006) report the first (and, so far, only convincing XMM-Newton-based) measurement of the black hole spin in an AGN: $a = 0.989\pm^{0.009}_{0.987}$ in MCG-6-30-15 (compare with the measurement of the black hole spin in our Galaxy discussed by Bernard Aschenbach in this volume using a different technique). More measurements are coming from the broadband X-ray spectra (0.5–200 keV) measured by *Suzaku* Schmoll et al. (2009); Miniutti et al. (2009). On the other hand, the detection of periodic or quasi-period modulations in the X-ray light curve may yield a measurement of the black hole mass fully independent from reverberation studies in the optical, if one assumes that the associated frequency is related to the dynamical timescales of the innermost regions in the illuminated accretion disk. This technique has been applied so far to the modulation of the relativistic iron line peak in NGC 3516 Iwasawa et al. (2004). The discovery of the first quasi-periodic oscillation (period of about 1 hour) in an AGN, RE J1034+396 Gierliński et al. (2008) could be used for the same purpose (or allow the identification of the QPO nature if the mass is independently known).

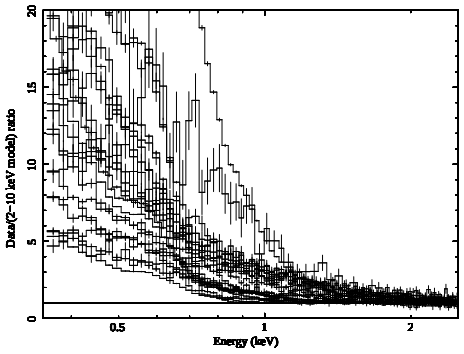

Fig. 2. EPIC-pn residuals (in units of data/model ratio) once the best-fit model in the 2–10 keV energy band is extrapolated down to 0.35 keV. The sources are all those in the CAIXA sample Bianchi et al. (2009) where the peak strength of the soft excess (in the aforementioned units) is comprised between 5 and 20 in the 0.35–2 keV energy band.

2.2. Soft excess in radio-quiet AGN

The solution of the relativistic issue may lead to the solution of another puzzle, which X-ray astronomers have striven to clarify, so far at no avail. It has been known since early observations with EXOSAT Turner & Pounds (1989) that the X-ray spectra of AGN exhibit an abrupt and smooth steepening below $\simeq$1 keV. This steepening has *grosso modo* the same smooth shape (although very different strength and steepness!) in AGN with a wide range of luminosities (Fig. 2), ruling out a simple explanation in terms of the blue tail of the Comptonized accretion disk. This interpretation would require a constant disk temperature over more then three orders of magnitude in black hole mass Gierliński & Done (2004), at odds with the expectations of the accretion disk theory Shakura & Sunyaev (1973). Once again, two main explanations compete for the heart of the X-ray astronomers, both of them advocating that the common phenomenological shape of the soft excess reflects the atomic physics rather then the AGN astrophysics: reflection from a relativistic ionised accretion disk Ross & Fabian (2005); Crummy et al. (2006), and absorption from a relativistically smeared high-ionisation, high-density, and high-velocity outflow Gierliński & Done (2004).

The former interpretation is naturally linked to the interpretation of the iron line red wing as due to relativistic effects. Stronger soft excess implies a larger relative normalisation of the disk reflection component to the primary continuum. In a lamppost geometry, this may be due to the high-energy source being located closer to the accretion disk plane. In this case, light bending effects become important, which yield a natural explanation for the lack of correlation between the intensity of the primary continuum and of the reflection features Miniutti & Fabian (2004); Ponti et al. (2006).

2.3. The quest for relativistic outflows

Evidence for the existence of relativistic outflows in AGN is mounting, thanks to the detection of deep, narrow, variable absorption features in the EPIC spectra of several AGN Pounds et al. (2003a,b); Risaliti et al. (2005); Cappi et al. (2009). In PDS 456 Reeves et al. (2003) - the brightest quasar in the local universe - a deep absorption edge at $\simeq$7.5–8.0 keV is the imprinting of an outflow with a ionisation parameter $\log(\xi) \simeq 4.5$, column density $\log(N_H) \geq 10^{24}$ cm^{-2}, and outflow velocity 0.1–0.3 c, launched at a distance of about 100 gravitational radii from the black hole. The outflow luminosity ($\sim 10^{47}$ erg s^{-1}) is of the order of the accreted and of the Eddington luminosity. The total integrated luminosity during the AGN duty-cycle ($\sim 10^{61-62}$ erg) is of the order of the binding energy of 10^{11} solar masses (assuming a dispersion velocity of 300 km s^{-1}) King & Pounds (2003). The possibility that such outflow could significantly affect the host galaxy dynamics as well as the chemical enrichment of the interstellar medium is being passionately discussed (see, *e.g.*, Krongold et al. 2007).

The discovery of semi-relativistic outflows in AGN besides the slower and more standard "warm absorbers" George et al. (1998); Blustin et al. (2005) should be no surprise for anyone: theoreticians tell us that high-velocity outflows are an inescapable by-product of re-

alistic magneto-hydrodynamic simulations of accretion disks Krolik et al. (2007); Proga (2007).

On a slightly critical (with the most accepted paradigm) note, XMM-Newton studies of large samples of AGN suggest that the strength of the soft excess is anti-correlated with the width of the H_β line Bianchi et al. (2009), confirming earlier ROSAT Boller et al. (1997) and ASCA Brandt et al. (1999) results.

2.4. Obscured AGN

In AGN covered by a column density of neutral gas larger then $\sim 10^{22}$ cm^{-2} the primary emission is totally suppressed below 2 keV, i.e. in the energy range where the RGS spectrometer is sensitive. These "obscured AGN" are, however, far from being X-ray silent. On the contrary, observations with the RGS (and with the grating instruments on board *Chandra*) have unveiled spectra rich in recombination lines of Carbon, Nitrogen, Oxygen, Neon, Magnesium and Silicium, as well as of L-shell transitions of Fexvii to Fexxi (see Fig. 3). The continuum is generally negligible. The best high-resolution spectrum of an obscured AGN ever taken is still an early XMM-Newton RGS exposure of NGC 1068 (the brightest obscured AGN in soft X-rays; Fig. 3) discussed by Kinkhabwala et al. (2002). Standard plasma diagnostics apply: the ratio between the components of the He-like Oxygen, Nitrogen and Neon triplets - where the forbidden component largely dominates over the intercombination and the resonant - is strongly indicative of photoionisation. The detection of narrow ($kT \simeq 4$ eV) radiative Recombination Continua Liedahl et al. (1995) allows to constrain the temperature of the plasma. The ratio between higher order transitions and the H-like Ly-α shows that resonant scattering plays an important role in the ionisation/excitation balance, and constraints the column density of the gas in the range $N_H = 10^{17-18}/Z_O$ cm^{-2}, where Z_O is the Oxygen abundance. This early results were later confirmed by RGS spectra of other bright obscured AGN such as Mkn 3 Bianchi et al. (2005); Pounds et al. (2005) and NGC 4151 Armentrout et al. (2007). In their study of a sample of about 90 Seyfert 2 RGS spectra presently available in the XMM-Newton science archive, Guainazzi & Bianchi (2007) showed that the conclusions derived from the detailed analysis of a few bright sources RGS spectra can be extended to the population of obscured AGN in the local universe. The association of line-rich soft X-ray spectra with extended emission on scales from hundreds of parsecs to a few kilo-parsecs Bianchi et al. (2006), and the morphological coincidence between the X-ray and O[iii] emission on these spatial scales Wilson et al. (2000); Young et al. (2001); Bianchi et al. (2006) suggest that the emitting region is located in the (Extended) Narrow Line Region.

2.4.1. The size of the X-ray source in NGC 1365: a detour

There rare a few exception, though. The most remarkable is NGC 1365. This galaxy is an example of "Changing-look" AGN Matt et al. (2003), exhibiting changes of the column density covering the active nucleus by almost one order of magnitude on a time scale as short as 2 days Risaliti et al. (2007). Assuming that the spectral change is due to the occultation of the X-ray source by a single cloud, one can constrain the size of the X-ray source to be $< 10^{13}$ cm, and the distance of the obscuring clouds $\sim 10^{16}$ cm. Similar "tomographic" experiments have been possible on a few other sources so far Elvis et al. (2004), in some cases thanks to XMM-Newton deep observations Puccetti et al. (2007). NGC 1365 also exhibits a peculiar RGS spectrum, dominated by collisionally ionised thermal plasma emission Guainazzi et al. (2009), most likely associated to clusters of star forming regions within about 3 kpc from the nucleus Wang et al. (2009). It is possible that this peculiar spectroscopic properties are due to shielding of the primary continuum by the same optically thick matter responsible for the extreme variability of the X-ray obscuring column density.

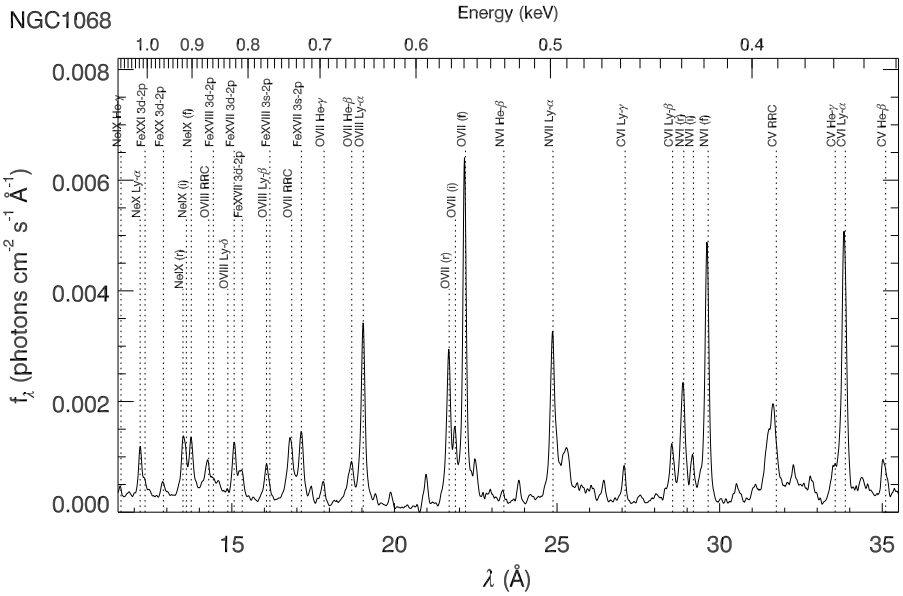

Fig. 3. RGS spectrum of NGC 1068 Kinkhabwala et al. (2002). Strong Ly-α lines from Nex, Oviii, Nvii and Cvi, the He-like triplets of Neix, Ovii, Nvi and Cvi and Radiative Recombination Continuum features of Oviii, Ovii and Cvi are clearly visible. The spectrum has been rebinned with a 5-channel triangular kernel for plotting purposes only.

2.5. Scaling laws between galactic and supermassive black holes

AGN are strongly variable X-ray sources Barr & Mushotzky (1986). Only recently, however, it has been possible to measure characteristic timescales in the range days to months Edelson et al. (1999); Uttley et al. (2002); McHardy et al. (2004) by joining deep XMM-Newton exposures with long photometric monitoring campaigns with RXTE. If these timescales are related to dynamical processes in the accretion disk, one may expect that they scale with the black hole mass. This has been recently proved to be true, once a correction due to the accretion rate is applied McHardy et ak. (2006). This correlation holds over more than eight orders of magnitudes in mass and three orders of magnitudes in accretion rate. This scaling law predicts also a correlation between the characteristic timescale and the width of the optical lines, used as a proxy for the velocity dispersion in the Broad Line Region (BLR). The optical line width is primarily driven by the viral motion of the gas clouds in the gravitational potential of the supermassive black hole ($v^2 \sim GM_{BH}/R_{BLR}$, where R_{BLR} is the inner radius of the BLR); in turn the size of the BLR is $\propto L^a \propto (M_{BH}\dot{m_{Edd}})^a$, with $a \simeq 0.5$. The combination of the above relations yields $v^4 \sim M_{BH}/\dot{m_{Edd}}$. The observed correlation between v and the characteristic timescale perfectly matches the predictions McHardy et ak. (2006).

2.6. AGN cosmological evolution

A substantial amount of XMM-Newton observing time is being spent on surveys of different sky coverage and depth. XMM-Newton main strength is the large collecting area of the EPIC cameras, which allows us to reach detection limits ~1–2×10^{-15} erg s^{-1} cm^{-2} Hasinger et al. (2001); Brunner et al. (2008), without being affected

by confusion in the hard X-ray band. Combining the XMM-Newton pencil-beam survey of the Lockman Hole Brunner et al. (2008) with *ROSAT* and *Chandra* surveys, Hasinger et al. (2005) could for the first time constrain the space density of soft X-ray selected AGN in the Seyfert luminosity regime ($L_X \leq 10^{43}$ erg s^{-1}), and detect a clear decline with redshift. The evolutionary behaviour of AGN shows a strong dependence on luminosity: the space density of high-luminous quasars peaks at $z \simeq 2$, whereas that of Seyfert galaxies peaks well below $z \simeq 1$. This has allowed to tighten the observation constraints on the Cosmic X-ray Background (CXB) synthesis models Gilli et al. (2007). Some of their implications are now uncontroversial. A luminosity dependent density evolution is consistent with soft X-ray selected Hasinger at el. (2005) as well as hard X-ray selected Ueda et al. (2003); La Franca et al. (2005); Barger et al. (2005) AGN surveys; the distribution of column density raises towards larger values, and a substantial contribution by Compton-thick sources is required to account for the CXB peak at 30 keV; the fraction of obscured AGN, F, decreases with luminosity (as originally pointed out by Lawrence & Elvis, 1982, and recently confirmed, among others, by results of XMM-Newton surveys La Franca et al. (2005); Akylas et al. (2006); Della Ceca et al. (2008). Whether F also depends on redshift is still a matter of debate.

3. Conclusions

We are living a "golden era" of X-ray astronomy. A fleet of operational observatories have allow giant leaps in our understanding of the X-ray universe and in our comprehension of the associated astrophysical processes. XMM-Newton has specifically contributed to this success with four "strengths"

- the largest (and so far unsurpassed) collecting area of its optics
- the large dynamical range of the exposure times (ranging from a few hours to weeks), well matching different timescales and source fluxes
- the unprecedented (and so far unsuppressed) high-resolution line detection power in the soft X-ray band
- the simultaneous optical-UV-X-ray coverage

In order to make a step forward, future X-ray mission shall be able to retain the XMM-Newton legacy, while improving in one or more of the following areas:

- improved energy resolution, and its extension to the whole X-ray band
- broad-band coverage of the hardest X-ray band
- high spatial resolution
- long-term monitoring and all-sky hard X-ray surveys

Some of these challenges will be met by the *International X-Ray Observatory*, a cooperation project among ESA, NASA and JAXA to launch the next large-mission class X-ray observatory in the 2020 time-frame, and whose study is currently ongoing. Jean Clavel presents the concept of this mission in this volume.

Acknowledgements. I thank Annalia Longinotti and Giovanni Miniutti for discussions, which led to an improvement of an early version of this manuscript, and for providing me with material prior to its publication.

References

Akylas A., Georgantopoulos I., Georgakis A., Kitsionas S., Hatziminaoglou E., 2006, A&A, 459, 693

Armentrout B.K., Kramer S.B., Turner T.J., 2007, ApJ, 665, 237

Barger A.J., Cowie L.L., Mushotzky R.F., et al., 2005, AJ, 129, 578

Barr P., Mushotzky R.F., 1986, Nat, 320, 421

Bianchi S., Guainazzi M., Chiaberge M., 2006, A&A, 448, 499

Bianchi S., Guainazzi M., Matt G., Fonseca Bonilla N., Ponti G., A&A, 2009, 495, 421

Bianchi S., Miniutti G., Fabian A.C., Iwasawa K., 2005, MNRAS, 360, 380

Blandford R.D. & Znajek R.L., 1977, MNRAS, 323, 506

Blustin A.J., Page M.J., Fürst S.V., et al., 2005, A&A, 431, 111
Boller T., Brandt W.N., Fabian A.C., Fink H.H., 1997, MNRAS, 289, 393
Brandt W.N., Boller T., Fabian A.C., Ruszkowski M., 1999, MNRAS, 303, L53
Brenneman L.W., Reynolds C.S., 2006, ApJ, 652, 1028
Brunner H., Cappelluti N., Hasinger G., et al., 2008, A&A, 479, 283
Cappi M., Tombesi F., Bianchi S., et al., 2009, A&A, 504, 401
Crummy J., Fabian A.C., Gallo L., Ross R.R., 2006, MNRAS, 365, 1067
Della Ceca R., Caccianiga A., Severgnini P., et al., 2008, A&A, 487, 119
den Herder J., et al., 2001, A&A, 365, L7
Dewangan G.C., et al., 2003, ApJ, 592, 52
Elvis M., Risaliti G., Nicastro F., Miller J.M., Fiore F., Puccetti S., 2004, ApJ, 615, L25
Edelson R. & Nandra K., 1999, ApJ, 514, 682
Fabian A.C., Rees M.J., Stella L., White N.E., 1989, MNRAS, 238, 729
Fabian A.C. & Vaughan S., 2003, MNRAS, 340, L28
Fabian A.C., Zoghbi A., Ross R.R., et al., 2009, Nat, 459, 540
George I.M., Turner T.J., Netzer H., Nandra K., Mushotzky R.F., Yaqoob T., 1998, ApJS, 114, 73
Gierliński M., Done C., 2004, MNRAS, 349, L7
Gierliński M., Middleton M., Ward M., Done C., 2008, Nat, 455, 369
Gilli R., Comastri A., Hasinger G., 2007, A&A, 463, 79
Guainazzi M., Bianchi S., 2007, MNRAS, 374, 1290
Guainazzi M., Risaliti G., Nucita A., et al., 2009, A&A, in press (arXiv:0908.0268)
Hasinger G., Altieri B., Arnaud M., et al., 2001, A&A, 365, L45
Hasinger G., Miyaji T., Schmidt M., 2005, A&A, 441, 417
Jansen F., Lumb D., Altieri B., et al., 2001, A&A 365, L1
King A.R., Pounds K.A., 2003, MNRAS, 345, 657
Kinkhabwala A., Sako M., Behar E., et al., 2002, ApJ, 575, 732
Krolik J.H., Hawley J.F., Hirose S., 2007, MxAC, 27, 1
Krongold Y., Nicastro F., Elvis M., et al., 2007, ApJ, 659, 1022
Iwasawa K., Miniutti G., Fabian A.C., 2004, MNRAS, 355, 1073
La Franca F., Fiore F., Comastri A., et al., 2005, ApJ 635, 864
Lawrence A. & Elvis M., 1982, ApJ, 256, 410
Liedahl D.A., Osterheld A.L., Goldstein W.H., 1985, ApJL, 438, 115
Markowitz A. Reeves J.N., Braito V., 2006, ApJ, 646, 783
Martocchia A., Matt G., Karas V., 2002, 383, L23
Mason K.O., Breeveld A., Much R., et al., 2001, A&A, 365, L36
Matt G., Guainazzi M., Maiolino R., 2003, MNRAS, 342, 422
Matt G., Perola G.C., Piro L., Stella L., 1992, A&A, 257, 63 (erratum: 263, 453)
McHardy I., Koerding E., Knigge C., Uttley P., Fender R.P., 2006, Nat, 444, 730
McHardy I., Papadakis I.E., Uttley P., Page M.J., Mason K.O., 2004, MNRAS, 348, 783
Miller J.M., 2007, ARA&A, 45, 441
Miller L., Turner T.J., Reeves J.N., 2007, A&A, 483, 437
Miniutti G., Fabian A.C., 2004, MNRAS, 349, 1435
Miniutti G., Panessa F., de Rosa A., et al., 2009, MNRAS, 398, 255
Nandra K., O'Neill P.M., George I.M., Reeves J.N., 2007, MNRAS, 382, 194
Ponti G., Miniutti G., Cappi M., Maraschi L., Fabian A.C., Iwasawa K., 2006, MNRAS, 368, 903
Pounds K., King A.R., Page K.L., O'Brien P.T., 2003b, MNRAS, 346, 1025
Pounds K.A., Page K.L., 2005, MNRAS, 360, 1123
Pounds K.A., Reeves J.N., King A.R., Page K.L., 2004, MNRAS, 350, 10
Pounds K., Reeves J.N., King A.R., Page K.L., O'Brien P.T., Turner M.J.L., 2003a, MNRAS, 345, 705
Proga D., 2007, ApJ, 661, 693
Puccetti S., et al., 2007, MNRAS, 377, 607

Reeves J., O'Brien P.T., Ward M., 2003, MNRAS, 593, L65
Reeves J.N., Nandra K., George I.M., Pounds K., Turner T.J., Yaqoob T., 2004, ApJ, 602, 648
Risaliti G., Bianchi S., Matt G., et al., 2005, ApJ, 630, L129
Risaliti G., Elvis M., Fabbiano G., Baldi A., Zezas A., Salvati M., 2007, ApJ, 659, L111
Risaliti G., Salvati M., Elvis M., et al., 2009, MNRAS, 393, L1
Ross R.R., Fabian A.C., 2005, MNRAS, 358, 211
Saxton R.D., Read A.M., Esquej P., Freyberg M.J., Altieri B., Bermejo D., 2008, A&A, 480. 611
Schmoll S., Miller J.M., Volonteri M., et al., ApJ, 703, 2171
Shakura N.I., Sunyaev R.A., 1973, A&A, 24, 337
Steenbrugge K., Kaastra J.S., Sako M. et al., 2005, A&A, 432, 453
Strüder L., Briel U., Dannerl K., et al., 2001, A&A 365, L18
Tanaka Y., Nandra K., Fabian A.C., et al., 1995, Nat, 375, 659
Trimble V., Ceja J.A., 2008, AN, 329, 632
Turner M.J.L., Abbey A., Arnaud M., et al., 2001, A&A 365, L27
Turner T.J., Miller L., 2009, A&ARv, 17, 47
Turner T.J., Mushotzky R.F., Yaqoob T., et al., 2002, ApJ, 574, L12
Turner T.J., Pounds K., 1989, MNRAS, 240, 833
Ueda Y., Akyama M., Ohta K., Miyaji T., 2003, ApJ, 559, 886
Uttley P., McHardy I., Papadakis I.E., 2002, MNRAS, 332, 231
Wang J., Fabbiano G., Elvis M., et al. 2009, ApJ, 694, 718
Watson M.G., Schröder A.C., Fyfe D., et al., 2009, A&A, 493, 339
Wilms J., Reynolds C.S., Begelman M.C., et al., 2001, MNRAS, 328, L27
Wilson A.S., Shopbell P.L., Simpson C., Storchi-Bergmann T., Barbosa F.K.B., Warm M.J., 2000, AJ, 120, 1325
Young A.J., Wilson A.S., Shopbell P.L., 2001, ApJ, 556, 6